Journal of Materials Chemistry A

Accepted Manuscript

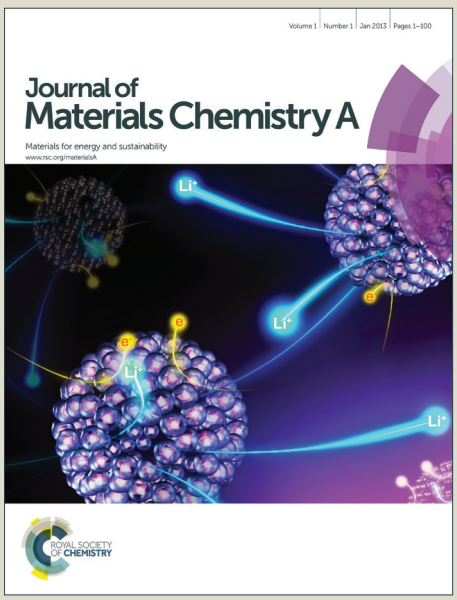

ROYAL SOCIETY OF CHEMISTRY

www.rsc.org/materialsA

Journal Name

ARTICLE

Thermo-processable covalent scaffolds with reticular hierarchical porosity and their high efficiency capture of carbon dioxide†

Received 00th January 20xx,
Accepted 00th January 20xx

DOI: 10.1039/x0xx00000x

www.rsc.org/

Su-Young Moon,‡ [a] Eunkyung Jeon,‡ [a] Jae-Sung Bae,[a] Mi-Kyoung Park,[b] Chan Kim,[c] Do Young Noh,[c] Eunji Lee[b] and Ji-Woong Park [a]*

The preparation of moldable porous organic scaffolds with a hierarchical pore structure is demonstrated and used for adsorption of carbon dioxide. The study shows for the first time that molecularly cross-linked covalent networks can be molded to a desired shape with three-dimensionally interconnected pores ranging over multiple length scales. Thermal cleavage and rearrangement chemistry of urea bonds allows the network to generate subnanometer pores while their nanoparticles being sintered to a monolithic structure containing pores of 2 to 100 nm via inter-particle sintering. Selective expulsion of small molecular fragments during the thermolysis of the network generated the reticular micropores. The resultant hierarchically porous objects exhibited excellent capacity and selectivity for adsorption of carbon dioxide even from low concentration sources, for example, from the gas mixture of the typical indoor air quality. The soft covalent network approach used here gives insights to the development of covalent organic networks with pore-based functionalities.

Introduction

Organic materials with pores smaller than a few nanometers are usually derived from rigid molecular building blocks via their covalent bonding to form a three-dimensional network.[1-5] These materials, with their pore size approaching molecular dimension, have the potential to be used for molecular storage and separation, [6-11] catalysts or catalyst supports,[12-18] and sensors.[12-15, 19-20] A variety of porous network materials with improved porosities and functionalities have been developed for absorption or adsorption-based separation of energy and environment-related molecular species. [21-27]

One of the main issues concerning the porous network of covalently bonded building blocks (referred to as a "covalent network") is to fabricate a hierarchical pore structure, i.e., a network consisting of interconnected pores of different sizes. For the large surface area of microporous materials to be efficiently utilized by adsorbing guest molecules, especially at a low partial pressure, it is essential to build mesoscale conduits and channels across the network to facilitate molecular transport. For example, it is possible to envisage a material with the structure in a microscopic scale resembling the hierarchical respiratory tree found in mammalian lungs. The poor processabilities of covalent networks, however, do not allow fabrication of such a hierarchical pore structure. New synthetic strategies allowing the formation of hierarchical pores through network materials have to be developed. In addition, developing a processable covalent network that can be fabricated in different shapes, such as beads, sheets, films, and monoliths, would enable the unique porosities of these networks to be exploited.[28-30]

Here we demonstrate that a soft, three-dimensional covalent network can be rearranged thermally, during which small molecular fragments can be selectively removed to generate molecular scale pores through the network. We also show that the network, composed of thermally reversible bonds, can be sintered and molded into a monolithic object of a desired shape from its nanoparticles. As a result, we create a moldable covalent network with reticulated micro-, meso-, and macropores that exhibits highly selective adsorption of carbon dioxide in high capacity even from low concentration sources.

Experimental details

Synthesis of urea-bonded network (UN)

Tetrakis(4-aminophenyl)methane (TAPM) (0.482 g, 1.263 mmol) was dissolved in N,N-dimethylformamide (DMF) (22.6 mL). 1,6-hexamethylenediisocyanate (HDI) (0.425 g 2.527 mmol) was added to the solution and the mixture was stirred at room temperature under nitrogen. After stirring for 60 h, the resulting sol was poured into a copious amount of acetone

[a] School of Materials Science and Engineering, Gwangju Institute of Science and Technology, 123 Cheomdan-gwagiro, Buk-gu, Gwangju, 500-712, Korea. jiwoong@gist.ac.kr
[b] Graduate School of Analytical Science and Technology, Chungnam National University, Daejon, 305-764, Korea.
[c] Department of Physics and Photon Science, Gwangju Institute of Science and Technology, 123 Cheomdan-gwagiro, Buk-gu, Gwangju, 500-712, Korea

† Electronic Supplementary Information (ESI) available: Synthetic and experimental methods, supplementary figures. See DOI: 10.1039/x0xx00000x

‡ Su-Young Moon and Eunkyung Jeon contributed equally to this work.

with continued stirring. The precipitates were collected by filtration and then stirred in acetone and filtered, a process that was repeated three times. The resulting powders were then dried under high vacuum at 150 °C for 24 h.

Thermal treatment of UN

UN powders were placed in a glass vial and heated to the desired temperature (230~380 °C) in an electric furnace at a rate of 2 °C min^{-1} under a constant 20 ml min^{-1} flow of nitrogen. The sample was held at this target temperature for 1 h. For preparation of molded monoliths, the original UN powders were placed in a mold and pressed with 10 tons for 5 min. The molded sample was treated using the same procedure as was used for the powders.

Results and Discussion

We had anticipated that a network consisting of urea bonds would be an ideal candidate for a rearrangeable soft network because a urea bond can be reverted to an amine and isocyanate as the temperature is elevated above 200°C (Fig. 1).[31-32] An important feature of urea chemistry is that thermally regenerated isocyanate groups become fused to form more stable isocyanurate rings, which provides a mechanism to reassemble a fragmented network (Fig. 1a).[32-34] Low-molar-mass fragments may be vaporized off as the urea network becomes fragmented, providing molecular-scale micropores to the remaining network (Fig. 1b). Furthermore, the reversible bond dissociation and recombination will allow sintering of neighboring objects of the urea network as shown in Fig. 1c. Sintering of nano-particulate networks would yield a three-dimensional monolithic framework with the generation of mesoscale pores as in the case of inorganic materials.[35-36] The method affords a thermally processable organic network-based materials with a hierarchical pore structure, which will exhibit enhanced molecular adsorption performances.

We prepared a urea-bonded network (UN) by cross-linking polymerization of tetrakis(4-aminophenyl)methane (TAPM) and 1,6-hexamethylenediisocyanate (HDI) by the organic sol-gel method that we developed recently.[37-38] Key to the current method is to prepare the network in nanoparticulate form. Spherical UN particles with diameters of 50-100 nm were readily produced by the sequence of mixing TAPM and HDI in N,N-dimethylformamide (DMF), adding the resulting sol into a nonsolvent, and then collecting the nanopowder precipitate (See Experimental section). Thermogravimetric analysis (TGA) of dry UN powders indicated that the sample started to lose weight at 250 °C, slightly higher than the temperature at which the urea bonds are known to break. We sought an optimum condition for the UN samples to rearrange to a structure exhibiting the highest possible porosity by varying the thermal treatment temperature. The sample was slowly heated to a rearrangement temperature (T_r) between 250 and 380°C.

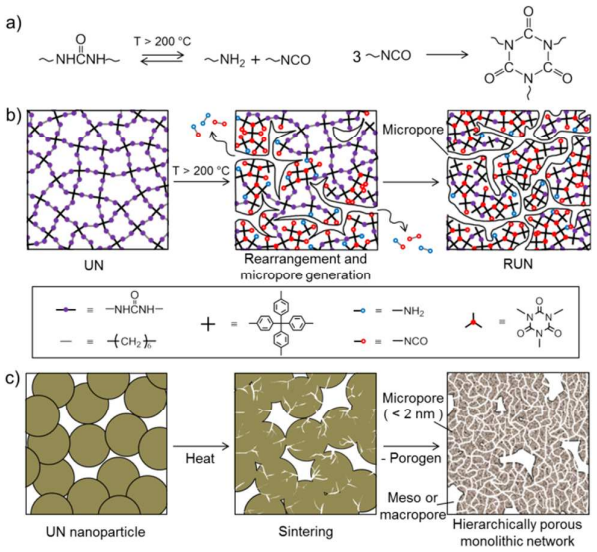

Fig. 1 Rearrangement of a soft covalent molecular network into a reticular hierarchically porous monolith. a) Dissociation of urea bonds of the network and subsequent cyclization of three isocyanate groups into an isocyanurate ring. b) Schematic representation of the rearrangement of a urea network with simultaneous generation of micropores. Fragmentation of the network is initiated from the surface of solid particles, where the bonds have a higher rotational freedom. The cleavage in the network propagates into the interior with the release of aliphatic fragments. Terminal isocyanate groups trimerize to form isocyanurate, resulting in the formation of a stable network with reticular micropores. c) Neighbouring particles are sintered to form a monolithic framework containing meso/macropores as well as micropores.

The nanopowders obtained by precipitation were readily molded to a disk-shaped sample by compression (Fig. 2). The molded UN disk shrunk upon thermal treatment while maintaining its original shape. The resulting disk was sufficiently sturdy against an applied pressure of as high as 50 bar. Transmission (TEM) and scanning (SEM) electron microscopy images of the rearranged UNs (RUNs) show that they indeed consisted of a three-dimensional framework containing mesopores throughout (Fig. 2d and 2e). Furthermore, high-magnification images of the framework skeletons showed relatively bright thread-like interconnected features, which are likely to be through-pores formed across the network. The pore width appeared to be on average smaller than a few nanometers (this was confirmed further by the analysis based on gas adsorption isotherms as described in the next section). The blank area in the TEM image for the ultrathin section (Fig. 2e) corresponds to the meso- or macropores present across the sintered framework, which can be also shown by the SEM image in Fig. 2d.

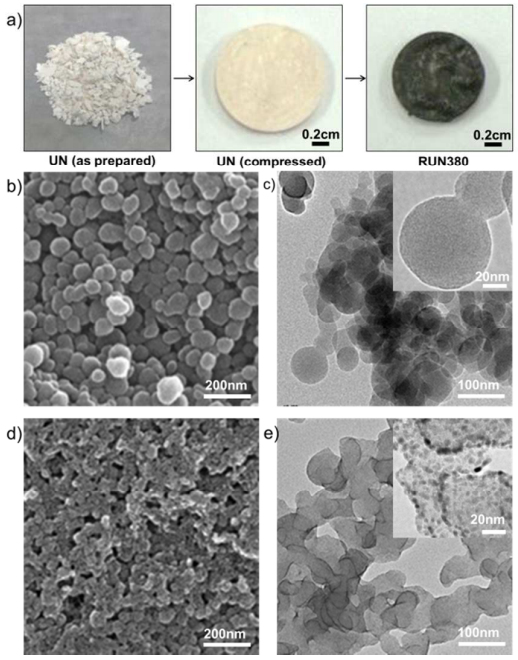

Fig. 2 The structure of the hierarchically porous framework of a rearranged urea network (RUN). a) Optical photographs of as-prepared UN powder, a disk prepared by compression of UN, and the disk of the resulting RUN treated at T_r =380°C (referred to as "RUN380"). b) SEM image of a fractured UN pellet. c) Cross-sectional TEM image of a UN pellet. d) SEM image of a fractured pellet of RUN380. e) Cross-sectional TEM image of an RUN380 pellet. The granules in b) transformed into the monolithic framework in d). Insets in c) and e) show high magnification TEM images, in which brighter thread-like features are present only in the RUN sample. Thin sections with a thickness of approximately 50 nm were obtained by using an ultra-microtome and then stained with RuO_4.

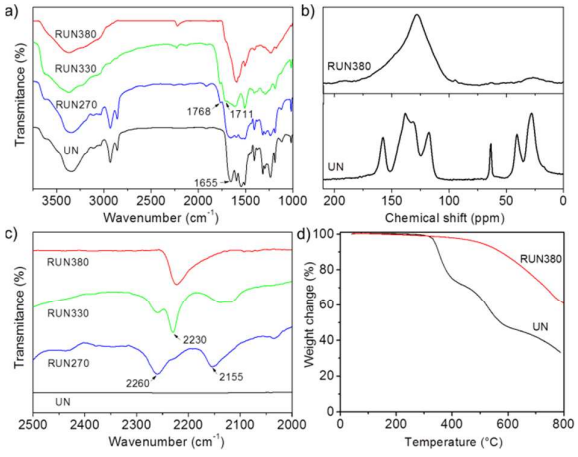

Fig. 3 The thermally induced chemical transformation of UN. a) FT-IR spectra of the UN and RUNs heated to different T_r values. The samples were heated to the T_r at a rate of 2 °C/min under a nitrogen atmosphere and then kept at the same temperature for 1 h. The arrows point the absorbance bands at 1655 cm^{-1}, 1711 cm^{-1} and 1768 cm^{-1} which correspond to carbonyl stretching vibrations for urea, isocyanurate and uretidinedione, respectively. b) ^{13}C CP/MAS spectra of RUN380 and UN. c) Magnified FT-IR spectra in the region of 2000~2500 cm^{-1} for UN and RUNs. The peaks at 2260 cm^{-1}, 2155 cm^{-1} and 2230 cm^{-1} are attributed to the isocyanate, carbodiimide, and cyanamide stretching vibrations, respectively, which were generated during thermal dissociation and rearrangement of urea bonds (See Figure 1S). d) Thermogravimetric analysis curves of UN and RUN380. They were acquired at a heating rate of 10 °C/min under a nitrogen flow of 20 ml/min.

Thermal treatment removed selectively the aliphatic portion of UNs, as evidenced by various experimental data. IR spectra of RUNs showed that the intensities of the C-H stretching bands at 2930-2860 cm^{-1} decreased with increasing T_r for the samples, becoming absent in the samples treated at temperatures higher than 350°C. The samples heated to intermediate rearrangement temperatures exhibited IR bands corresponding to isocyanate, carbodiimide and cyanamide as well as isocyanurate which are known to be generated during thermolysis of urea or urethane bonds. The peaks at 2260cm^{-1}, 2155cm^{-1} and 2230cm^{-1} are attributed the isocyanate, carbodiimide and cyanamide stretching vibrations, respectively. The carbonyl stretching vibrations for urea, isocyanurate and uretidinedione appeared at 1655cm^{-1}, 1711cm^{-1} and 1768 cm^{-1}, respectively (Fig. 3a, 3c and Fig. S1).[39-40] Solid-state ^{13}C NMR spectra of the RUN samples indicate the absence of aliphatic segments (Fig. 3b), consistent with the IR analysis. The condensates collected at the outlet of the thermolysis chamber consisted mainly of aliphatic fragments according to our analysis of the ^{1}H NMR spectra (Fig. S2). X-ray photoelectron spectroscopy (XPS) of the RUN treated at T_r =380°C (referred to as "RUN380") yielded data consistent with the removal of aliphatic segments and the formation of isocyanurates (Fig. S3 and Table S1). Once the aliphatic segments were completely removed, the RUN sample did not show a significant loss of weight up to 500°C (Fig. 3d).[41]

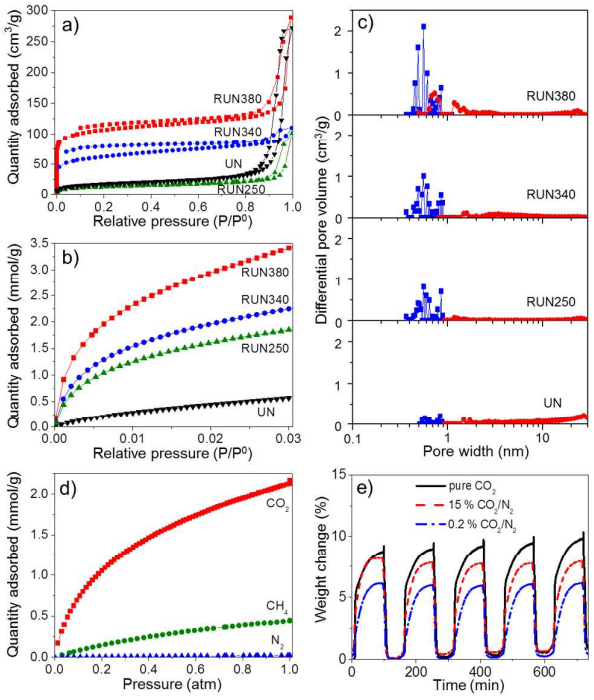

Fig. 4 Porosity and gas adsorption characteristics of RUNs. a) N_2 adsorption isotherms acquired at 77 K for UN and for RUNs formed at three different T_r values (250 °C, 340 °C and 380 °C). b) CO_2 adsorption isotherms acquired at 273 K for UN and these RUNs c) Pore-size distribution (See Fig. S6 for magnified view) derived from combined adsorption data of N_2 and CO_2 for the RUNs. d) Gas adsorption curves acquired at 298 K for CO_2, CH_4 and N_2 with RUN380. e) Repeated CO_2 adsorption and desorption curves with RUN380. A stream of feed gas was made to flow into the TGA sample chamber at 25°C for adsorption; then the sample was heated to 100°C for desorption.

A strong IR band near 3400 cm^{-1} for this RUN (Fig. 3a) shows that it still contained a significant number of urea bonds, while broadening of entire IR spectrum suggests that each part of the networks became more tightly connected after thermal rearrangement. The IR spectra of the RUN indicates that chemical functional groups can be maintained in the structure thanks to the moderate temperature range of thermal modification. Broad D and G peaks in the Raman spectra and broad powder x-ray diffraction curve for the RUNs are indicative of the formation of amorphous carbon (Fig. S5), but elemental analysis shows that the bulk of RUN sample was enriched with nitrogen and oxygen atoms (Table S2). The RUNs consist mainly of the urea or isocyanurate network that would result from UN upon removal of aliphatic segments.[42] High N and O content of the RUNs is distinct from conventional carbonized materials. Specific chemical functionalities may be inserted to any RUN scaffold by addition of the monomer or comonomer with the corresponding chemical structure into the organic sol-forming mixtures.

The evolution of the pore structure by thermal rearrangement was clearly revealed from the nitrogen adsorption isotherms (Fig. 4a). These curves show that the RUNs, but not the UN, exhibited micropore filling at low pressures. The surface area, as calculated by the BET equation, increased as the T_r was increased, and was calculated to be 402 m^2/g for RUN380, which was likely due to the micropores (<2 nm) created during the thermal rearrangement. The adsorption capacity of RUN380 for carbon dioxide (3.6 mmol/g at 1 bar) is six times greater than that of untreated UN (0.6 mmol/g at 1 bar) (Fig. 4b). The CO_2 adsorption of RUN380 is comparable to or higher than that of other known porous organic materials (Table S3).[6, 18, 43-44] Density function theory (DFT)-based pore size analysis using both the CO_2 and N_2 adsorption curves indicates that RUNs have pores with a wide distribution of sizes, including micropores (<2 nm) as well as meso- and macropores with widths ranging from 2 to 100 nm (Fig. 4c and Fig. S6). Fig. 4c indicates that the total quantity of micropores with widths less than 2 nm increased as T_r was increased. RUNs exhibited high CO_2 uptake, even at room temperature, with excellent selectivity over N_2 (Fig. 4d).The adsorption selectivity of RUN380 for CO_2 over N_2 in flue gas (15 wt% CO_2/N_2) and that over CH_4 in natural gas (10 wt% CO_2/CH_4) compositions at 298K and 1 bar were estimated to be 186 and 15, respectively, by applying ideal adsorbed solution theory (IAST) along with the pure component isotherm fits (Fig. S7 and Table S4).[45-46] This high selectivity is attributed to the high heats of adsorption of the RUN for CO_2, estimated to be in the range of 35~45 kJ/mol (Fig. S8). The CO_2/N_2 and CO_2/CH_4 adsorption selectivity of RUN380 were also estimated from the initial slopes of single-gas adsorption isotherms to be 477 and 10, respectively (Fig. S9). These values are comparable to or greater than those of other porous polymer networks[3] or metal organic frameworks (MOFs).[47] Indeed, RUN shows excellent CO_2 adsorption selectivity and capacity for gas mixtures with low concentration CO_2 as expected from the single gas adsorption data. Gravimetrically determined CO_2 capture capacities of RUN380 from pure, 15%, and 2000 ppm CO_2 mixed with N_2 were 9, 8, and 6 wt% respectively, and these values persisted over multiple adsorption-desorption cycles (Fig. 4e). It is remarkable that the RUNs could take up to about 6 wt% from a source containing only 2000 ppm CO_2. Conclusions

We have demonstrated the synthesis of thermo-processable, hierarchically porous covalent organic scaffolds. After synthesizing nanoparticulate urea-based networks using the organic sol-gel method, we then showed that the urea network can be rearranged thermally, while expelling small porogenic molecular fragments, to generate highly microporous scaffolds. The reversible chemistry also allowed sintering of the covalent network, transforming the powdery network materials to monoliths. The resulting organic scaffolds possess hierarchical porosity with three-dimensionally interconnected micro-, meso- and macropores. These structures adsorb carbon dioxide with high selectivity and a high capacity, and are thus promising materials for carbon dioxide capture technology. We expect our soft network approach to provide insights into developing porous polymeric and organic materials with even greater applicability for molecular separation and storage.

Acknowledgements

S. –Y. Moon and E. Jeon contributed equally to this work. This work was supported by the Korea CCS R&D Center (KCRC) grant funded by the Korea government (Ministry of Science, ICT & Future Planning) (2014M1A8A1049265).

Notes and references

1 H. M. El-Kaderi, J. R. Hunt, J. L. Mendoza-Cortés, A. P. Côté, R. E. Taylor, M. O'Keeffe and O. M. Yaghi, *Science*, 2007, **316**, 268-272.
2 N. B. McKeown and P. M. Budd, *Macromolecules*, 2010, **43**, 5163-5176.
3 W. Lu, D. Yuan, J. Sculley, D. Zhao, R. Krishna and H.-C. Zhou, *J. Am. Chem. Soc.*, 2011, **133**, 18126-18129.
4 R. Dawson, A. I. Cooper and D. J. Adams, *Prog. Polym. Sci.*, 2012, **37**, 530-563.
5 E. Delebecq, J.-P. Pascault, B. Boutevin and F. Ganachaud, *Chem. Rev.*, 2013, **113**, 80-118.
6 R. Dawson, E. Stockel, J. R. Holst, D. J. Adams and A. I. Cooper, *Energ. Environ. Sci.*, 2011, **4**, 4239-4245.
7 C. D. Wood, B. Tan, A. Trewin, F. Su, M. J. Rosseinsky, D. Bradshaw, Y. Sun, L. Zhou and A. I. Cooper, *Adv. Mater.*, 2008, **20**, 1916-1921.
8 P. Nugent, Y. Belmabkhout, S. D. Burd, A. J. Cairns, R. Luebke, K. Forrest, T. Pham, S. Ma, B. Space, L. Wojtas, M. Eddaoudi and M. J. Zaworotko, *Nature*, 2013, **495**, 80-84.
9 Z. Chang, D.-S. Zhang, Q. Chen and X.-H. Bu, *Phys. Chem. Chem. Phys.*, 2013, **15**, 5430-5442.
10 P. Arab, M. G. Rabbani, A. K. Sekizkardes, T. İslamoğlu and H. M. El-Kaderi, *Chem. Mater.*, 2014, **26**, 1385-1392.
11 S.-Y. Moon, E. Jeon, J.-S. Bae, M. Byeon and J.-W. Park, *Polym. Chem.*, 2014, **5**, 1124-1131.
12 P. Kaur, J. T. Hupp and S. T. Nguyen, *ACS Catal.*, 2011, **1**, 819-835.
13 H. Qian, J. Zheng and S. Zhang, *Polymer*, 2012, **54**, 557-564.

14 S.-Y. Ding, J. Gao, Q. Wang, Y. Zhang, W.-G. Song, C.-Y. Su and W. Wang, *J. Am. Chem. Soc.* , 2011, **133**, 19816-19822.
15 J. S. Seo, D. Whang, H. Lee, S. I. Jun, J. Oh, Y. J. Jeon and K. Kim, *Nature*, 2000, **404**, 982-986.
16 R. K. Totten, Y.-S. Kim, M. H. Weston, O. K. Farha, J. T. Hupp and S. T. Nguyen, *J. Am. Chem. Soc.* , 2013, **135**, 11720-11723.
17 S. Pandiaraj, H. B. Aiyappa, R. Banerjee and S. Kurungot, *Chem. Commun.*, 2014, **50**, 3363-3366.
18 P. Pachfule, V. M. Dhavale, S. Kandambeth, S. Kurungot and R. Banerjee, *Chem. Eur. J*, 2013, **19**, 974-980.
19 W. Luo, Y. Zhu, J. Zhang, J. He, Z. Chi, P. W. Miller, L. Chen and C.-Y. Su, *Chem. Commun.*, 2014, **50**, 11942-11945.
20 C. Gu, N. Huang, J. Gao, F. Xu, Y. Xu and D. Jiang, *Angew. Chem. Int. Ed.*, 2014, **53**, 4850-4855.
21 Y.-Q. Shi, J. Zhu, X.-Q. Liu, J.-C. Geng and L.-B. Sun, *ACS Appl. Mater. Interfaces*, 2014, **6**, 20340-20349.
22 Q. Chen, D.-P. Liu, J.-H. Zhu and B.-H. Han, *Macromolecules*, 2014, **47**, 5926-5931.
23 J.-X. Hu, H. Shang, J.-G. Wang, L. Luo, Q. Xiao, Y.-J. Zhong and W.-D. Zhu, *Ind. Eng. Chem. Res.*, 2014, **53**, 11828-11837.
24 S. Wu, Y. Liu, G. Yu, J. Guan, C. Pan, Y. Du, X. Xiong and Z. Wang, *Macromolecules*, 2014, **47**, 2875-2882.
25 G. Li, B. Zhang, J. Yan and Z. Wang, *J. Mater. Chem. A*, 2014, **2**, 18881-18888.
26 J. Wang, S. Xu, Y. Wang, R. Cai, C. Lv, W. Qiao, D. Long and L. Ling, *RSC Adv.*, 2014, **4**, 16224-16232.
27 S.-Y. Ding and W. Wang, *Chem. Soc. Rev.*, 2013, **42**, 548-568.
28 S. Furukawa, J. Reboul, S. Diring, K. Sumida and S. Kitagawa, *Chem. Soc. Rev.*, 2014, **43**, 5700-5734.
29 A. Ahmed, M. Forster, R. Clowes, P. Myers and H. Zhang, *Chem. Commun.*, 2014, **50**, 14314-14316.
30 J. W. Colson, A. R. Woll, A. Mukherjee, M. P. Levendorf, E. L. Spitler, V. B. Shields, M. G. Spencer, J. Park and W. R. Dichtel, *Science*, 2011, **332**, 228-231.
31 S. Caruso, S. Foti, P. Maravigna and G. Montaudo, *J. Polym. Sci. Pol. Chem. Ed.*, 1982, **20**, 1685-1696.
32 E. Delebecq, J.-P. Pascault, B. Boutevin and F. Ganachaud, *Chem. Rev.*, 2012, **113**, 80-118.
33 A. Lapprand, F. Boisson, F. Delolme, F. Méchin and J. P. Pascault, *Polym. Degrad. Stabil.*, 2005, **90**, 363-373.
34 R. E. Buckles and L. A. McGrew, *J. Am. Chem. Soc.* , 1966, **88**, 3582-3586.
35 S. Chang, R. H. Doremus, L. S. Schadler and R. W. Siegel, *Int. J. Appl. Ceram. Tec.*, 2004, **1**, 172-179.
36 D. Gebauer, X. Liu, B. Aziz, N. Hedin and Z. Zhao, *CrystEngComm*, 2013, **15**, 1257-1263.
37 S.-Y. Moon, J.-S. Bae, E. Jeon and J.-W. Park, *Angew. Chem. Int. Ed.*, 2010, **49**, 9504-9508.
38 S.-Y. Moon, H.-R. Mo, M.-K. Ahn, J.-S. Bae, E. Jeon and J.-W. Park, *J. Polym. Sci. A Polym. Chem.*, 2013, **51**, 1758-1766.
39 H. G. Khorana, *Chem. Rev.*, 1953, **53**, 145-166.
40 W. C. Schneider, *J. Am. Chem. Soc.* , 1950, **72**, 761-763.
41 M. Moritsugu, A. Sudo and T. Endo, *J. Polym. Sci. A Polym. Chem.*, 2011, **49**, 5186-5191.
42 Q. Wang, F. Cao and Q. Chen, *Green Chem.*, 2005, **7**, 733-736.
43 H. Furukawa and O. M. Yaghi, *J. Am. Chem. Soc.* , 2009, **131**, 8875-8883.
44 T. Ben, C. Pei, D. Zhang, J. Xu, F. Deng, X. Jing and S. Qiu, *Energ. Environ. Sci.*, 2011, **4**, 3991-3999.
45 A. L. Myers and J. M. Prausnitz, *AIChE. J.*, 1965, **11**, 121-127.
46 S. Xiang, Y. He, Z. Zhang, H. Wu, W. Zhou, R. Krishna and B. Chen, *Nat. Commun.*, 2012, **3**, 954.
47 E. D. Bloch, D. Britt, C. Lee, C. J. Doonan, F. J. Uribe-Romo, H. Furukawa, J. R. Long and O. M. Yaghi, *J. Am. Chem. Soc.* , 2010, **132**, 14382-14384.

Journal Name

ARTICLE

Graphical abstract and text

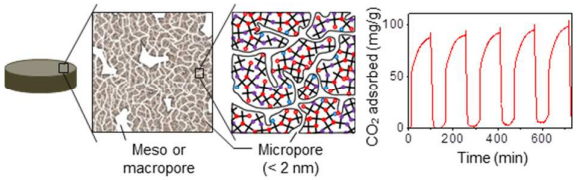

Hierachically porous organic network-based scaffolds comprised of reticulated micro-, meso, and macropores were demonstrated for high efficiency capture of carbon dioxide

Please do not adjust margins